

Theoretical Study of $1\Sigma^+$ States of Alkali Hydride XH Molecule (X = Na, K and Rb) in Adiabatic and Nonadiabatic Representations

Neji Khelifi*

King Saud University, College of Science Physics and Astronomy Department,
PO Box 2455, Riyadh 11451, Saudi Arabia

Received: April 30, 2009; Revised Manuscript Received: May 23, 2009

In this work, we present an adiabatic and nonadiabatic study for all the $1\Sigma^+$ states dissociating below the ionic limits [i.e., Na (3s, 3p, 4s, 3d, 4p, 5s, 4d, 4f), K (4s, 4p, 5s, 3d, 5p, 4d, 6s, 4f) and Rb (5s, 5p, 4d, 6s, 6p, 5d, 7s, 4f) + H (1s)]. The ab initio calculations rely on pseudopotential, operatorial core valence correlation and full valence CI (configuration-interaction) approaches, combined to an efficient diabatization procedure. For the low-lying states, our vibrational level spacings and spectroscopic constants are in good agreement with the available experimental data. Nonadiabatic potentials and dipole moments are analyzed, revealing the strong imprint of the ionic state in the $1\Sigma^+$ adiabatic states, while improving the results. This paper can be used as theoretical support for experimental work.

1. Introduction

Alkali hydrides have been the object of intense theoretical and experimental interest for many years.^{1–12} Such molecules are at the intersection of various theoretical and experimental challenges, and now are tractable with high reliability via ab initio techniques. Using appropriate methods, it is possible to approach the experimental results with an overall good agreement for the ground and excited states. Their ground state is known to be of ionic character but dissociates to neutral fragments.

A charge-transfer crossing is therefore expected to occur, making this problem attractive for diabatization. The nonadiabatic approach brings physical insight as shown in the previous studies of the LiH molecule,^{1,13,14} suggesting further calculations of non Born–Oppenheimer effects such as transitions occurring in collisions,^{15–17} estimation of vibronic effects (vibronic shifts and nonradiative lifetime).^{12,18–20} In addition, the nonadiabatic picture can be used to improve the accuracy of calculations, by overcoming basis set limitations on the electron affinity of H, which is among the main limitations in the ab initio approach, particularly for the binding energy of the ground state.¹ Undulations in the potential of the highly excited states were revealed and analyzed in the previous study of LiH¹ and further confirmed in various recent works.^{11,21–23} These undulations were shown to be magnified in the nonadiabatic curves and to be related to intrinsic characteristics of the Rydberg atomic functions.

Although realistic all-electron calculations are now feasible for the XH (X = Na, K, Rb) molecule, we prefer to use the pseudopotential approach for the core and large basis sets for the valence and Rydbergs states, which allows accurate descriptions of the highest excited states for the whole alkali hydride series. The two electrons are then treated at the full configuration-interaction level (here CISD: singles–doubles configuration interaction). Core–valence correlation effects are quite important. Here we used the well-established operatorial approach proposed by Müller, Flesh, and Meyer.²⁴ This paper presents the first ab initio calculations on highly excited states

of the XH alkali hydride molecule (X = Na, K, Rb), treating nearly all states dissociating below the ionic one [Na (3s, 3p, 4s, 3d, 4p, 5s, 4d, 4f), K(4s, 4p, 5s, 3d, 5p, 4d, 6s, 4f) and Rb (5s, 5p, 4d, 6s, 6p, 5d, 7s, 4f)]. The accuracy of the results can be judged by a comparison with the numerous theoretical and experimental data for the two lowest states. In addition to the adiabatic potential curves and dipoles moments, nonadiabatic curves are also derived. A further interest of this work is an improvement of both potential curves and dipole moments related to the H electron affinity correction effects allowed by the use of an efficient diabatization method. Therefore a rather complete set of data is presented about the XH (X = Na, K, Rb) molecule from ground to highly excited states including adiabatic potential energy in $1\Sigma^+$ and permanent dipole and transition dipole moments, as well as potential electronic couplings, for the corresponding nonadiabatic states. This set of data will be further used to perform detailed spectroscopic studies including vibronic effects, radiative and nonradiative life times.

In section 2 we briefly present the computational method and give numerical details. Section 3 is devoted to the presentation and discussion of the nonadiabatic and adiabatic results. Section 4 presents the permanent dipole moment for the adiabatic and nonadiabatic representations. Suggestions of spectroscopic interest are proposed in section 5. Finally, we summarize our results and conclude in section 6.

2. Methods

2.1. Computational Details. The alkali (sodium, potassium and rubidium) is treated as a one-electron system using the nonempirical pseudopotential of Barthelat and Durand,²⁵ in its semilocal form,⁴ and as in LiH¹ we used the abinitio package developed in Toulouse. We have used basis set 6s/5p/4d/2f for Na atom, 8s/5p/5d/2f for K atom and 8s/6p/6d/3f for Rb atom, where diffuse orbital exponents have been optimized to reproduce all the (3s, 3p, 4s, 3d, 4p, 5s, 4d, and 4f) atomic states for Na, (4s, 4p, 5s, 3d, 5p, 4d, 6s and 4f) atomic states for K and (5s, 5p, 4d, 6s, 6p, 5d, 7s and 4f) atomic states for Rb, while a more restricted basis set has been employed for hydrogen.

* E-mail: khelifineji@yahoo.fr.

TABLE 1: Optimized Cut-Off Parameters and Core Polarizability of X Atom (X = Na, K, Rb)

	ρ_s	ρ_p	ρ_d	ρ_f	α_{X^+} (bohr) ³
sodium Na	1.4423	1.625	1.5	1.5	$\alpha_{Na^+} = 0.993$
potassium K	2.115	2.1125	1.98	2.0	$\alpha_{K^+} = 5.457$
rubidium Rb	2.5095	2.2735	2.4978	2.51	$\alpha_{Rb^+} = 9.075$

TABLE 2: Calculated Transition Energies of the X Atom (X = Na, K, Rb)

atom	state	this work	expt ²⁷
Na	3s	0	0
	² P(3p)	16967.32	16968.0
	² S(4s)	25741.45	25740.0
	² D(3d)	29137.362	29137.0
	² P(4p)	30272.27	30271.0
	² S(5s)	33206.86	33201.0
	² D(4d)	34562.33	
	² F(4f)	34611.93	
	PI	41449.65	41438
K	4s	0	0
	² P(4p)	13023.6	13030.1
	² S(5s)	21014.1	21026.8
	² D(3d)	21535.3	21535.3
	² P(5p)	24717.5	24716.0
	² D(4d)	27401.9	27397.4
	² S(6s)	27446.2	27450.7
	² F(4f)	28142.2	28127.7
	IP	34998.2	35009.8
Rb	5s	0	0
	² P(5p)	12737.2	12737.2
	² D(4d)	19355.0	19355.0
	² S(6s)	20133.5	20097.5
	² P(6p)	23777.0	23775.9
	² D(5d)	25702.2	25702.5
	² S(7s)	26311.3	26292.8
	² F(4f)	26791.9	26801.1

This 5s, 3p, 2d basis set can be considered as a reasonable compromise, able to describe both neutral and negatively charged (H^-) hydrogen. A larger basis set for H could not be used because of numerical problems during the diabaticization process, the main effect of this rather small H basis being an error (405 cm^{-1}) in the H electron affinity, which however is corrected due to the nonadiabatic approach used. An extensive range of internuclear distances has been considered, ranging from 2.45 to 500 bohr, in order to cover all the ionic-neutral crossings in the $^1\Sigma^+$ symmetry. For the simulation of the interaction between the polarizable X^+ (X = Na, K, Rb) core with the valence electrons and H nucleus a core polarization potential is used, according to the operatorial approach of Müller, Flesh, and Meyer.²⁴ Following the formulation of Foucrault, Millie, and Daudey²⁶ cutoff functions with l -dependent adjustable parameters are fitted to reproduce not only the first experimental ionization potential but also the lowest excited states of each l , namely, [²S(3s), ²P(3p), ²D(3d) and ²F(4f)] for Na, [²S(4s), ²P(4p), ²D(3d) and ²F(4f)] for K and [²S(5s), ²P(5p), ²D(4d) and ²F(4f)] for Rb. In the present work, the core polarizability of alkali and the optimized cutoff parameters are given in Table 1. The resulting atomic spectra are reported in Table 2 for X (Na, K and Rb) atom (in cm^{-1}). The neutral dissociation limits reach a good accuracy for all the 3s, 3p, 4s, 3d, 4p, 5s, 4d and 4f states for Na atom, 4s, 4p, 5s, 3d, 5p, 4d, 6s and 4f states for K atom and 5s, 5p, 4d, 6s, 6p, 5d, 7s and 4f states for Rb atom, the largest error being 36 cm^{-1} .

2.2. Diabatization. We briefly recall the principal lines of the method used; more details can be found in previous

publications.^{1,29–31} The strategy is to compute a numerical estimate of the nonadiabatic coupling between the relevant adiabatic states and to cancel it by an appropriate unitary transformation according to the effective Hamiltonian theory.^{28,31}

The estimate is however obtained using the large internuclear intervals used in the molecular calculation instead of infinitesimal ones, and an effective overlap matrix is employed, in order to asymptotically ensure vanishing radial couplings and to get stable results. This nonadiabatic coupling calculation is closely related to an overlap matrix^{29,30} between the R -dependent adiabatic multiconfigurational states and an R_0 fixed set of reference states.

This diabaticization method was shown to be among the most effective for molecular ab initio calculations.³² The set of reference states are the nonadiabatic states calculated for the larger neighboring distance. The calculation is performed from the largest distance where the nonadiabatic states are initialized to the adiabatic ones to the shortest one, similar to an integration scheme. This method leads to smaller residual couplings between the nonadiabatic states.³³

3. Results

3.1. Nonadiabatic Results. The results are presented in Figures 1a, 1b and 1c, for the singlet Σ^+ states. As expected, the ionic curve crosses all the neutral Σ^+ states at different distances. For NaH, the crossing occurs with the 3s state around 8.0 bohr, with the 3p around 13.0 bohr, and with the 4s around 23.5 bohr. For KH, the crossing occurs with the 4s state around 8 bohr, with the 4p around 13 bohr, and with the 5s around 26.5 bohr. For RbH, the crossing occurs with the 5s state around 8.5 bohr, with the 5p around 15 bohr, and with the 4d around 25.5 bohr, the others occurring at much larger distances. Inspection of the coupling magnitude corroborates the conclusion (evident from the adiabatic curves) that the crossings become less and less avoided as the ionic curve asymptotically encounters higher-energy Rydberg states at increasing internuclear distances.

In Figures 1a, 1b and 1c, the ionic curve downshifted in energy by the H electron affinity error is also reported as a dotted line while the crossings with the neutral states are pushed to larger distances. As expected, the ionic curve behaves as $1/R$ at large internuclear distances, with some corrections proportional to $1/R^4$ corresponding to H^- dipolar polarization and also to core–valence interactions. The slope of the neutral curves seems erratic, but their nonadiabatic character, which should preserve intrinsic aspects of the Rydberg states, helps the analysis. As in LiH,¹ the apparently strange behavior of the nonadiabatic states can thus be satisfactorily interpreted by simple arguments, emphasizing again the physical relevance and utility of the diabaticization procedure.

3.2. Adiabatic Results and Corrections. Figures 2a, 2b and 2c illustrate the adiabatic curves of $^1\Sigma^+$ states for the three molecules. From the nonadiabatic picture, it is clear that the deep well of the ground state clearly results from the large avoided crossing between the ionic and the 3s state. Similarly to LiH, the first excited adiabatic $A^1\Sigma^+$ state presents a large well formed by the repulsive part of the [3s (Na), 4s (K) and 5s (Rb)] curves at short internuclear distance, a branch of the ionic curve at intermediate distance and the [3p (Na), 4p (K) and 5p (Rb)] asymptotes at large distances.

In contrast with LiH, the second excited state (C) presents a single minimum, at large internuclear distance, around the avoided crossing between the repulsive part of the 3p state and the ionic one. The third (D) and fourth (E) adiabatic $^1\Sigma^+$ states

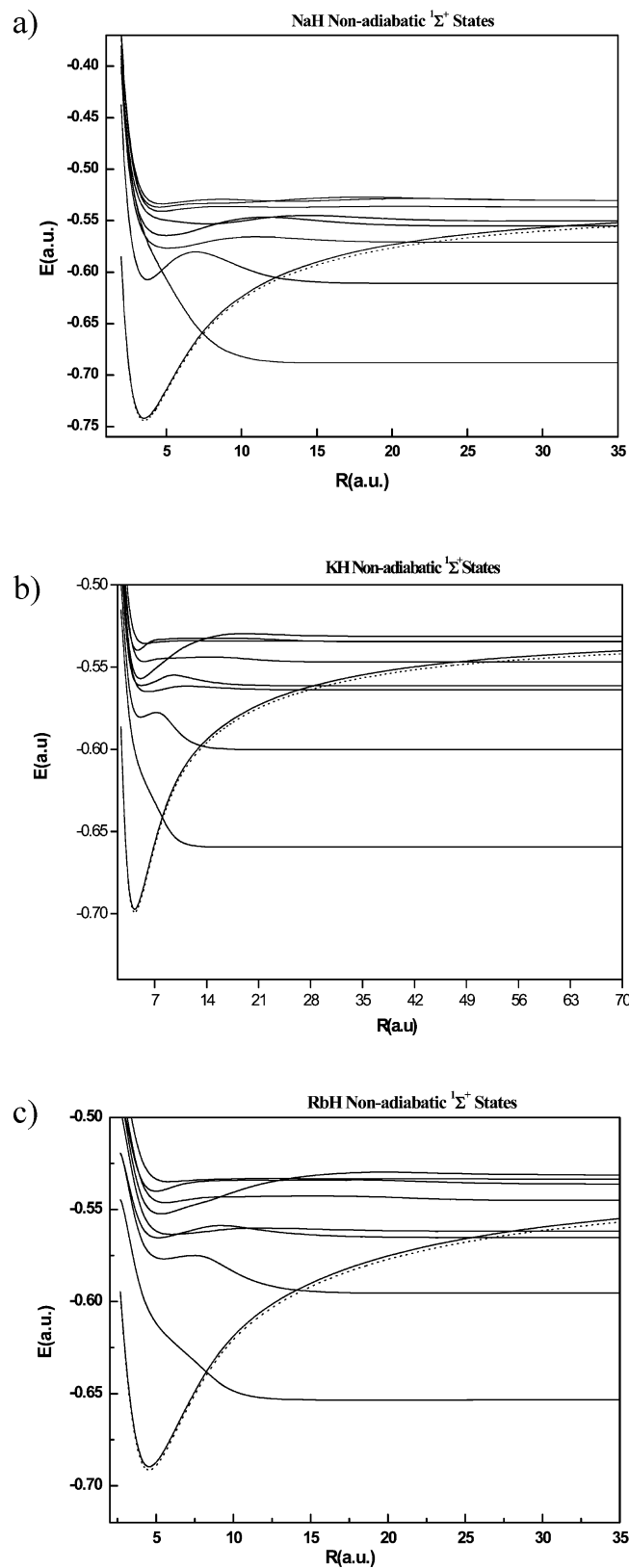


Figure 1. (a) NaH nonadiabatic potential energy curves for the $^1\Sigma^+$ states. (b) KH nonadiabatic potential energy curves for the $^1\Sigma^+$ states. (c) RbH nonadiabatic potential energy curves for the $^1\Sigma^+$ states.

present double minima, with a well at very large distances and another one at short distance in the Franck–Condon region of the ground state. Both minima can trap vibrational states. The crossings of the covalent and ionic states and the magnitude of their interaction completely determine the details of these adiabatic states and the resulting vibrational levels.

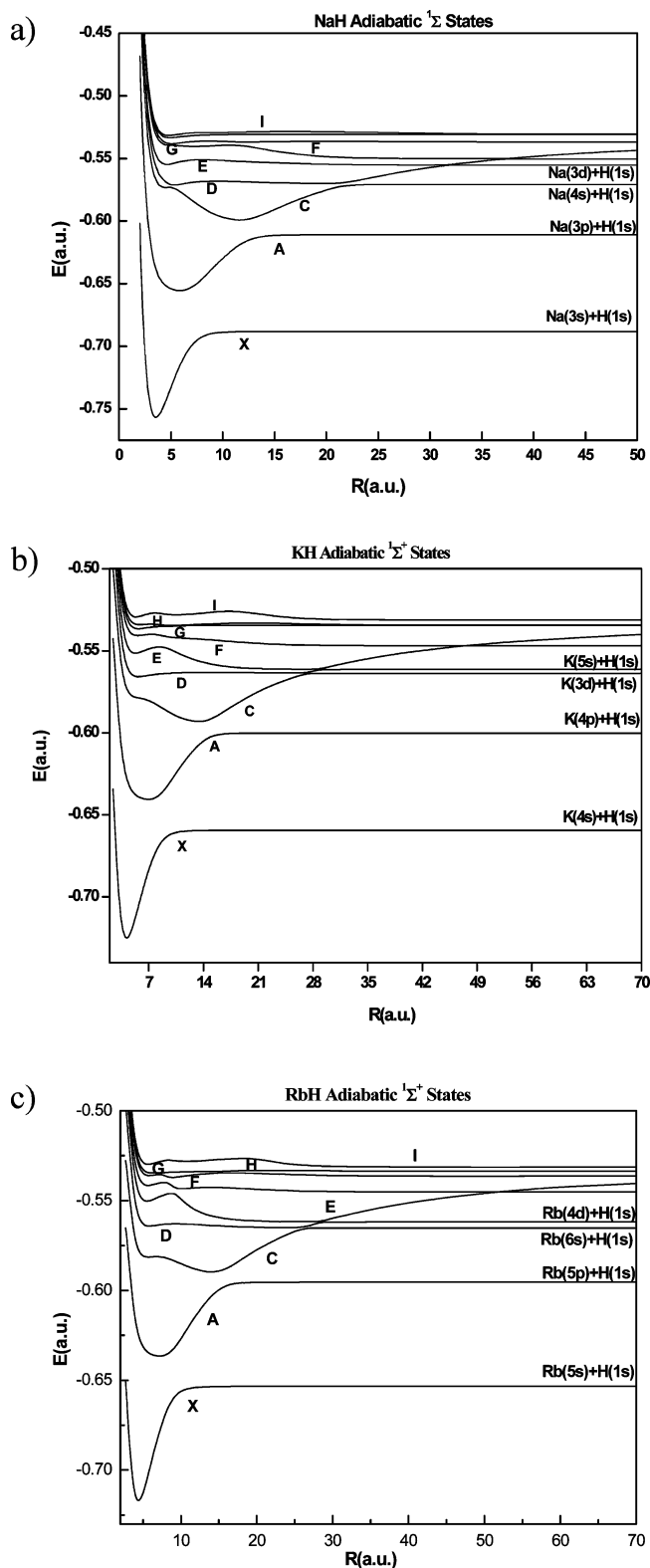


Figure 2. (a) NaH adiabatic potential energy curves for the $^1\Sigma^+$ states. (b) KH adiabatic potential energy curves for the $^1\Sigma^+$ states. (c) RbH adiabatic potential energy curves for the $^1\Sigma^+$ states.

In Figures 3a, 3b and 3c, the $^1\Sigma^+$ adiabatic states resulting from the diagonalization of the nonadiabatic effective Hamiltonian using the ionic curve corrected for the H electron affinity error are shown with dotted lines together with the previous adiabatic results. Although only the ionic potential has been modified, almost all adiabatic curves are affected, illustrating again their strong imprint due to the ionic state. Moreover, a

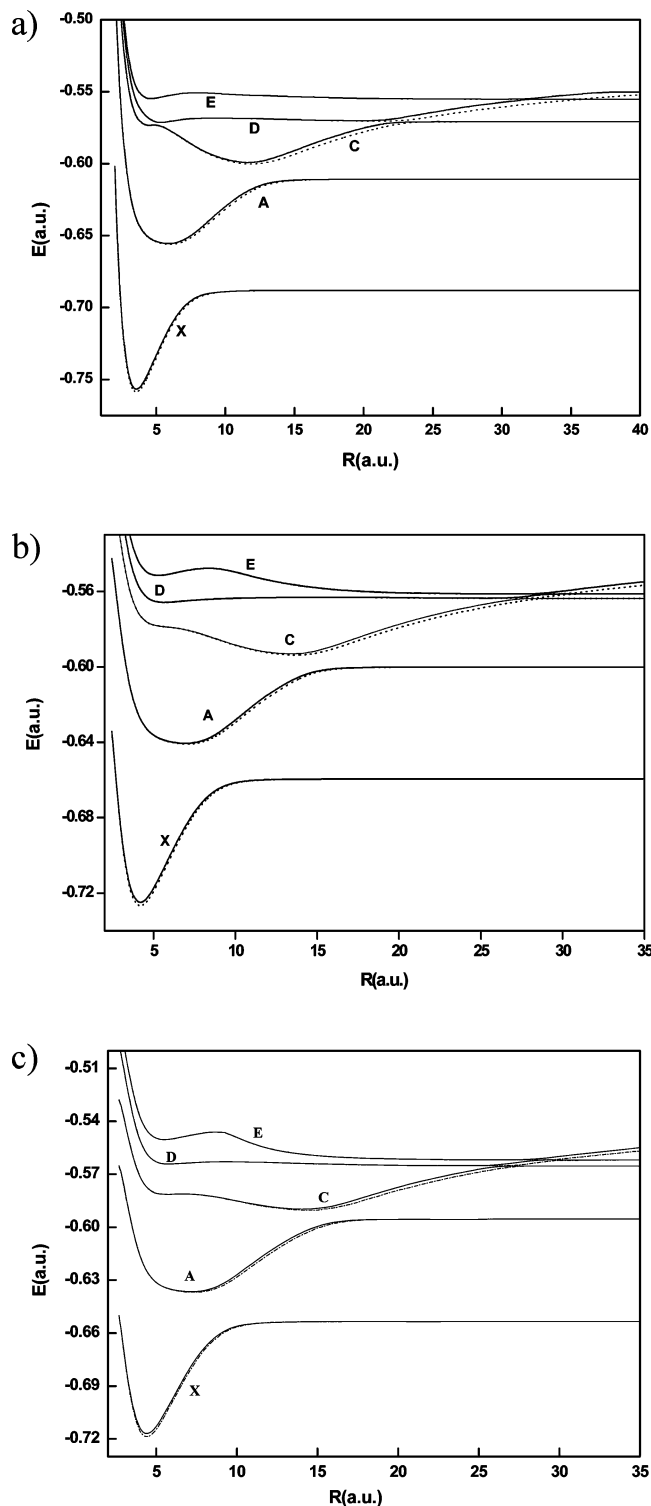


Figure 3. (a) NaH adiabatic potential energy curves for the $X^1\Sigma^+$, $A^1\Sigma^+$, $C^1\Sigma^+$, $D^1\Sigma^+$ and $E^1\Sigma^+$ states with (dotted line) and without (solid line) constant electroaffinity correction of hydrogen. (b) Same as Figure 3a but for KH molecule. (c) Same as Figure 3a but for RbH molecule.

difference between the two curves (full line and dotted line) locates a region where the adiabatic state is strongly ionic. The well of the ground state is downshifted in energy while the ones of the A and higher states are enlarged. These results which use an improved ionic potential will be referred to as improved results. It is interesting to examine how the improvement taking into account of the nonadiabatic representation modifies the spectroscopic constants of the $^1\Sigma^+$ states reported in Tables 3,

TABLE 3: Bond Distances R_e (au) and Dissociation Energies D_e (cm^{-1}) for the $X^1\Sigma^+$ State

molecule	refs	R_e (au)	D_e (cm^{-1})
NaH	<i>a</i>	3.507	15489.1896
	<i>b</i>	3.567	15798.6983
	ref 35	3.55	15683.0
	ref 38	3.558	15502.0
	expt ¹⁰	3.5659	15900 \pm 100
KH	<i>a</i>	4.19	14365.0
	<i>b</i>	4.19	14750.4
	ref 7	4.28	13954.1
	ref 34	4.29	12905.6
	ref 35	4.22	15066.6
RbH	expt ¹⁰	4.23	14772.7
	<i>a</i>	4.40	13940.0
	<i>b</i>	4.40	14323.2
	ref 7	4.49	14196.0
	ref 36	4.40	14397.0
ref 37	4.51	13227.0	
expt ¹⁰	4.47	14580.0	

^a Uncorrected ab initio results. ^b Improved results including correction of H electroaffinity of XH molecule (X = Na, K, Rb).

TABLE 4: Bond Distances R_e (au) and Dissociation Energies D_e (cm^{-1}) for the $A^1\Sigma^+$ State

molecule	refs	R_e	D_e
NaH	<i>a</i>	5.957	10011.4032
	<i>b</i>	6.056	10022.7156
	ref 35	6.01	9997.0
	ref 38	5.992	9993.0
	expt ¹⁰	6.0346	10137.0
KH	<i>a</i>	6.93	8872.9
	<i>b</i>	7.05	8946.3
	ref 34	7.18	8711.2
	ref 7	6.947	8711.2
	ref 35	7.01	8811.0
RbH	expt ¹⁰	7.11	8698.0
	<i>a</i>	7.20	9034.9
	<i>b</i>	7.30	9107.6
	ref 7	6.92	8711.2
	expt ¹⁰	7.30	8941.0

^a Uncorrected ab initio results. ^b Improved results including correction of H electron affinity of XH molecule (X = Na, K, Rb).

4, 5a, 5b and 5c. The binding energy of the ground state (Table 3) is considerably improved due to the correction of the ionic curve, indicating that the hydrogen electron affinity is an important parameter in the quality of ab initio calculations for the alkali hydrides. For the A state (Table 4) this correction improves the equilibrium distance which is underestimated in the uncorrected ab initio calculation. For higher excited states, no experimental data exist.

As can be seen in Tables 3 and 4, our improved results for the binding energy and the equilibrium distance are in good agreement with the experimental data,¹⁰ being better than older theoretical results and comparable to the most recent ones. Compared to the experimental results, our equilibrium distances are slightly too low because we use pseudopotentials and operator core–valence correlation estimates; some repulsive effects are clearly underestimated in our calculations. For better accuracy, pseudopotentials with smaller cores should be used.

As can be seen in Tables 6 and 7, this correction has no significant effect on the vibrational progression of the ground state since the whole potential curve (mainly ionic) has been slightly down shifted, except for the highest levels, close to the avoided crossing and where the improved results agree better with the experimental spacings. However, for the $A^1\Sigma^+$ state

TABLE 5: Bond Distances R_e (au), Dissociation Energies D_e (cm^{-1}) and Transition Energy T_e (cm^{-1}) for the Higher Excited $^1\Sigma^+$ States

state	refs	R_e (au)	D_e (cm^{-1})	T_e (cm^{-1})
(a) NaH Molecule ^a				
$C^1\Sigma^+$		4.542	575.437	44951.436
$D^1\Sigma^+$		5.263	3618.6716	48469.801
$E^1\Sigma^+$		4.630	1019.0337	49970.06
$F^1\Sigma^+$		7.189	1424.3087	53306.13
$G^1\Sigma^+$		5.061	350.2353	54541.83
$H^1\Sigma^+$		4.929	642.5400	55083.054
$I^1\Sigma^+$		4.774	277.51137	55233.88
(b) KH Molecule ^b				
$C^1\Sigma^+$		13.63	6584.5	34602.9
	ref 35	13.40	6516	
$D^1\Sigma^+$		5.65	873.5	38393.9
	ref 35	5.59	881.	
$E^1\Sigma^+$		5.28	1026.9	41217.0
	ref 35	5.24	1012.	
$F^1\Sigma^+$		5.57	1319.9	43475.5
	ref 35	5.49	1253.	
$G^1\Sigma^+$		5.67	459.5	44846.7
	ref 35	5.60	416.	
$H^1\Sigma^+$		5.83	768.7	45556.5
	ref 35	9.64	718.5	
		5.73	546.	
		10.30	660.	
$I^1\Sigma^+$		5.37	408.15	46161.4
	ref 35	5.41	233.	
(c) RbH Molecule ^c				
$C^1\Sigma^+$		5.65	3545.9	30132.7
		14.4	5509.2	28169.4
$D^1\Sigma^+$		5.77	504.3	33916.7
$E^1\Sigma^+$		5.5	1153.9	36947.3
$F^1\Sigma^+$		5.6	1133.3	38893.2
$G^1\Sigma^+$		5.8	515.5	40100.8
$H^1\Sigma^+$		6.2	699.6	40426.
$I^1\Sigma^+$		5.6	150.4	41459.6

^a Only the improved results (b) are reported of NaH molecule.

^b Only the improved results (b) are reported of KH molecule. ^c Only the improved results (b) are reported of RbH molecule.

only the long-range ionic branch is changed, and the well is enlarged, producing a lowering of all vibrational level spacings by several cm^{-1} .

Without any correction, almost all our vibrational level spacings ($E_{v+1} - E_v$) were larger than the experimental ones, indicating that the ionic branch was not attractive enough. With the correction, the vibrational level spacings are now almost all slightly lower than the experimental ones, indicating that the ionic curve becomes somewhat too attractive and the correction somewhat too large. As shown in Table 7, the experimental results for the $A^1\Sigma^+$ state are bracketed by our results with and without the constant correction, showing that the H electron affinity provides the dominant residual error.

4. Adiabatic and Nonadiabatic Permanent and Transition Dipole Moments

4.1. Permanent Dipole Moment. The permanent dipole moments are illustrated in Figures 4a, 4b and 4c for the adiabatic and in Figures 5a, 5b and 5c for the nonadiabatic $^1\Sigma^+$ states of XH molecule. We considered a large range of internuclear distances because we expected interesting features to arise from a global picture also involving the highly excited states, which become ionic at large internuclear distances. For the dipole of the ionic nonadiabatic state, we get an almost straight line, while

TABLE 6: Vibrational Level Spacings ($E_{v+1} - E_v$) of the $X^1\Sigma^+$ state of XH (X = Na, K, Rb) Molecule

molecule	v	this work without AEH	this work with AEH	expt ¹⁰	
NaH	1	1087.824	1118.135	1133.1017	
	2	1096.956	1080.184	1095.1108	
	3	1067.95	1043.82	1057.7626	
	4	1028.201	1008.148	1020.9757	
	5	988.537	972.932	984.6421	
	6	949.832	937.854	948.627	
	7	912.146	903.043	912.7686	
	8	876.763	868.233	876.8785	
	KH	1	911.253	914.21	955.868
		2	883.946	886.82	926.065
		3	856.946	860.18	896.888
		4	830.717	834.13	868.255
		5	805.039	808.54	840.153
		6	779.672	783.31	812.54
		7	754.559	758.42	785.339
		8	729.785	733.84	758.444
		9	705.106	709.56	731.744
		10	680.534	685.48	705.104
		11	655.833	661.46	678.358
12		630.765	637.3	651.286	
13		605.072	612.84	623.592	
14		578.331	587.77	594.883	
15		550.148	561.05	564.641	
16		519.896	531.54	532.169	
17		486.787	500.65	496.525	
18		449.698	467.33	456.525	
RbH		19	407.191	428.67	410.117
	20	357.286	384.98	355.393	
	21	297.609	332.67	289.629	
	22	225.324	270.01	210.233	
	23	139.124	194.32	115.623	
	1	866.494	863.672	908.79	
	2	841.331	838.164	881.12	
	3	816.558	813.005	853.93	
	4	792.073	788.179	827.23	
	5	767.908	763.774	801.03	
	6	744.054	739.688	775.3	
	7	720.561	715.961	750.07	
	8	697.47	692.475	725.33	
	9	674.677	669.224	707.07	
	10	652.049	646.132	677.31	

the permanent dipole of the neutral nonadiabatic states rapidly drops to zero as the internuclear distance increases.

This behavior is nicely consistent with a purely ionic nonadiabatic state and confirms the validity of our diabaticization approach on the basis of this physical property. For the adiabatic representation, we observe that, one after the other, each adiabatic state has its dipole that reaches the curve and then drops to zero. When combined, these curves reproduce piecewise the whole R curve characteristic of the ionic dipole and cross forming nodes between consecutive pieces. The curves seem to relay each other to this R line. This particular behavior can be easily understood from the nonadiabatic potential and dipole curves.

The permanent dipole gives actually a direct illustration of the ionic character of the adiabatic electronic wave function. We thus access directly a visualization of the R -dependence of the charge distribution of the wave function. The distance for which two consecutive adiabatic states have the same dipole locates the crossing of the ionic nonadiabatic state with the corresponding neutral one. The sharpness of the slopes around the node for the dipole is closely related to the weakness of the avoided crossing for energy.

Here again, taking benefit of the nonadiabatic representation it is possible to improve the results. Without any modification

TABLE 7: Vibrational Level Spacings ($E_{v+1} - E_v$) of the $A^1\Sigma^+$ State of XH (X = Na, K, Rb) Molecule

molecule	v	this work without AEH	this work with AEH	expt ¹⁰
NaH	1	325.837	321.81	323.63
	2	332.737	327.868	330.39
	3	339.078	334.318	337.23
	4	345.578	340.37	343.64
	5	351.355	345.645	349.26
	6	356.328	349.871	353.84
	7	360.017	352.801	357.25
	8	362.156	354.688	359.45
	9	362.80	355.538	360.47
	10	362.159	355.381	360.37
	11	360.547	354.396	359.31
	12	358.103	352.642	357.42
	13	355.026	350.232	354.84
	14	351.476	347.242	351.73
	15	347.56	343.687	348.2
	16	343.237	339.553	344.29
	17	338.51	334.91	340.02
	18	333.376	329.804	335.31
	19	327.808	324.273	329.96
	20	321.778	318.313	323.69
KH	1	246.36	241.41	236.09
	2	254.57	247.69	247.78
	3	263.64	256.06	257.83
	4	272.06	264.28	266.39
	5	279.24	271.24	273.56
	6	285.07	277.35	279.46
	7	289.63	281.92	284.18
	8	293.02	285.69	287.82
	9	295.35	288.16	290.47
	10	296.72	289.12	292.22
	11	297.24	290.68	293.15
	12	296.99	290.86	293.32
	13	296.09	290.23	292.82
	14	294.59	289.12	291.69
	15	292.56	287.44	290
	16	290.07	285.29	287.79
	17	287.16	282.8	285.11
	18	283.87	279.84	282
	19	280.22	276.62	278.49
	20	276.24	273.06	274.6
	21	271.93	269.16	270.36
	22	267.28	265.03	265.79
	23	262.26	260.54	260.88
	24	256.82	255.7	255.65
	25	250.9	250.53	250.09
	26	244.38	244.89	244.19
RbH	1	222.584	227.358	223.88
	2	230.25	237.035	234.62
	3	239.107	247.055	244
	4	248.051	255.972	252.09
	5	255.434	263.54	258.93
	6	261.738	269.622	264.64
	7	266.727	274.431	269.26
	8	270.524	278.01	272.87
	9	273.414	280.528	275.55
	10	275.27	282.16	277.37
	11	276.414	282.94	278.39
	12	276.783	283.013	278.71
	13	276.539	282.446	278.38
	14	275.743	281.316	277.49

of the dipole moment matrix in the nonadiabatic representation, but using now the previously determined nonadiabatic-adiabatic unitary transformation which involves the corrected ionic curve, we get improved results for the permanent and transition dipole moments.

The improved permanent dipoles for the X, A, C, D and E states are illustrated in Figures 6a, 6b and 6c with dotted lines,

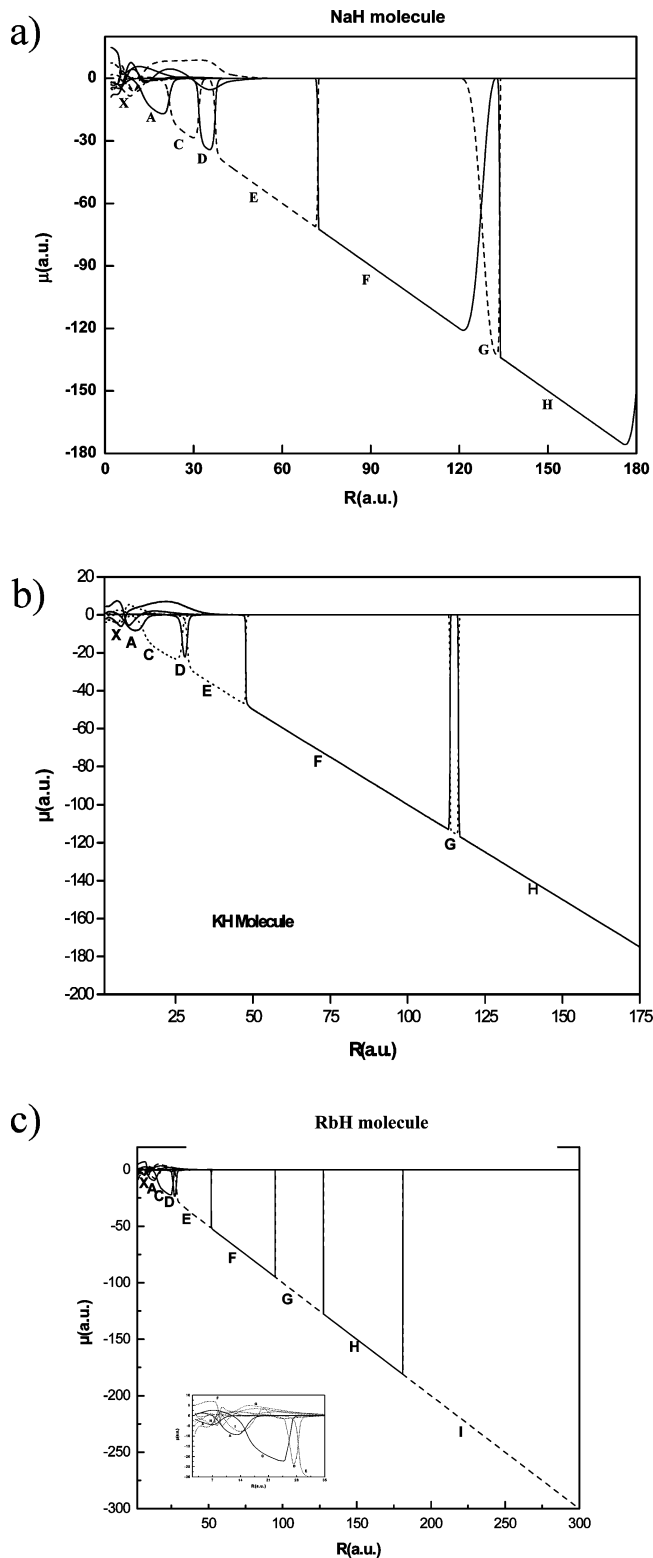


Figure 4. (a) Permanent dipole moments (μ) for the eight low-lying $1\Sigma^+$ states of the NaH molecule, as a function of the internuclear distance. Alternating solid and dashed lines correspond to X, A, C, D, E, F, G and H states. (b) Same as panel a but for KH molecule. (c) Same as panel a but for RbH molecule.

together with the direct ab initio results. The results are consistent with the previous analysis, the crossings being shifted to larger internuclear distances. Interestingly, since the experimental level spacing of the A state is bracketed by our results with and without the correction of the ionic curve, it can be expected that the exact permanent dipoles are also bracketed

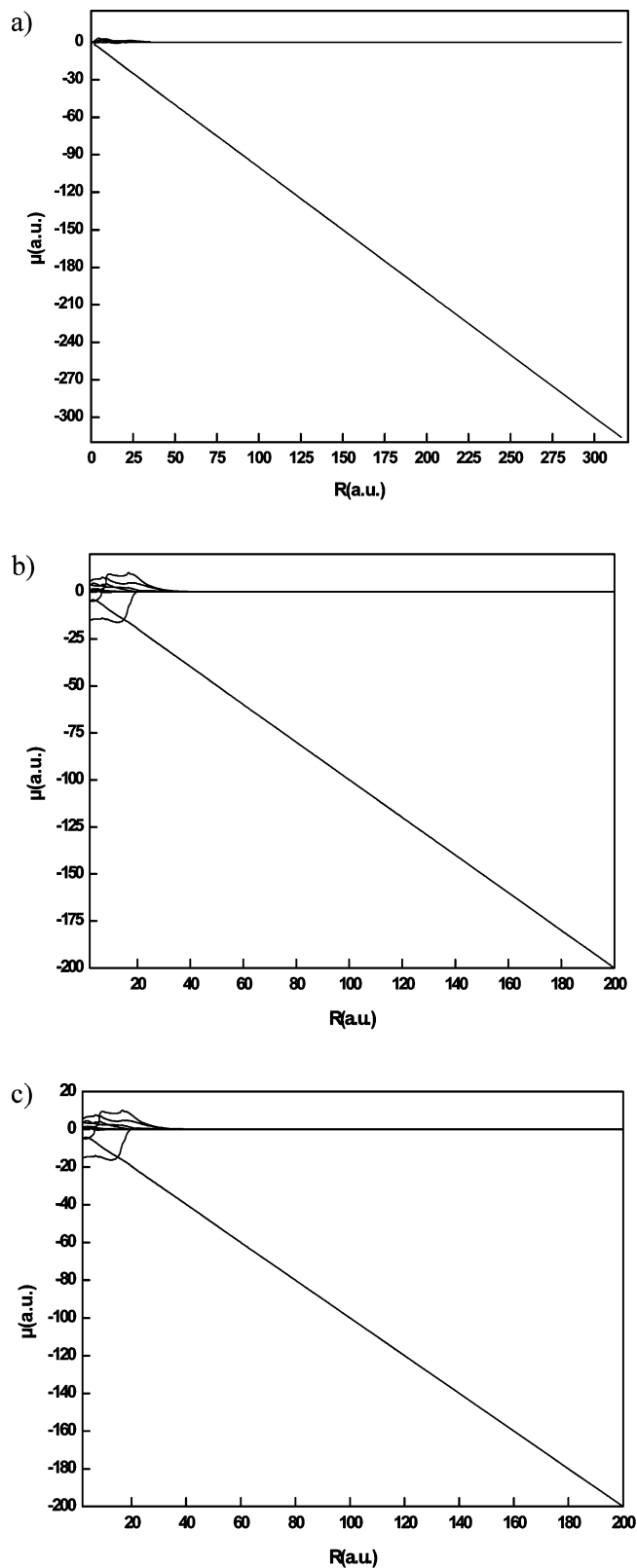


Figure 5. (a) Permanent nonadiabatic dipole moment for the eight low-lying $^1\Sigma^+$ states of the NaH molecule, as a function of the internuclear distance (all in au). (b) Same as panel a but for KH molecule. (c) Same as panel a but for RbH molecule.

by the full and dotted lines reported in Figures 6a, 6b and 6c, lying closer to the improved results (dotted lines).

4.2. Transition Dipole Moment. It is also interesting to illustrate the behavior of the transition dipole moments in the adiabatic representation. All of them cannot be shown here since

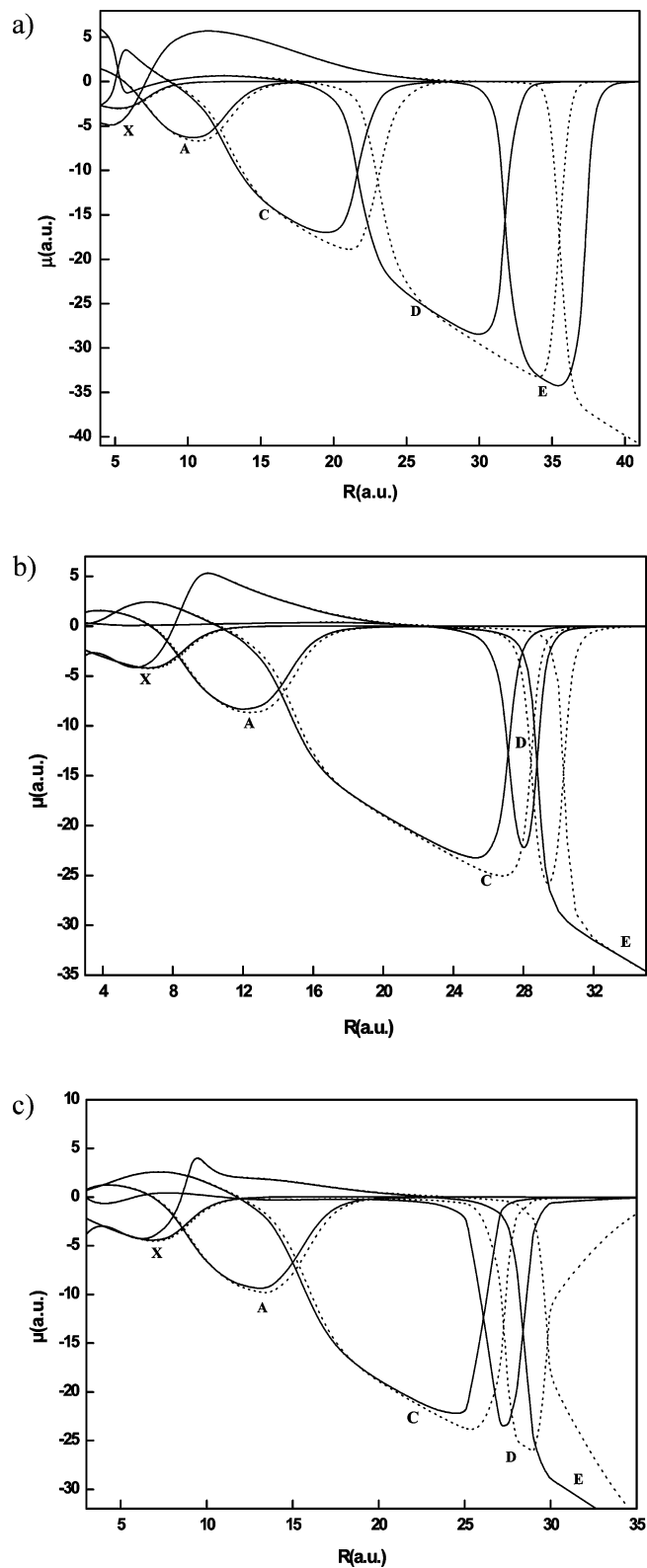


Figure 6. (a) Adiabatic permanent dipole moment X, A, C and D with (dotted line) and without (solid line) hydrogen electronic affinity correction of the NaH molecule, as a function of the internuclear distance (all in au). (b) Same as panel a but for KH molecule. (c) Same as panel a but for RbH molecule.

there are $n(n-1)/2$ curves, with $n=9$ for the $^1\Sigma^+$ states. Since the adiabatic states present strong variations of their physical electronic characteristics while the nonadiabatic states do not, it is not easy to follow their physical insight with a very restricted number of states. Adiabatic transition dipole moments

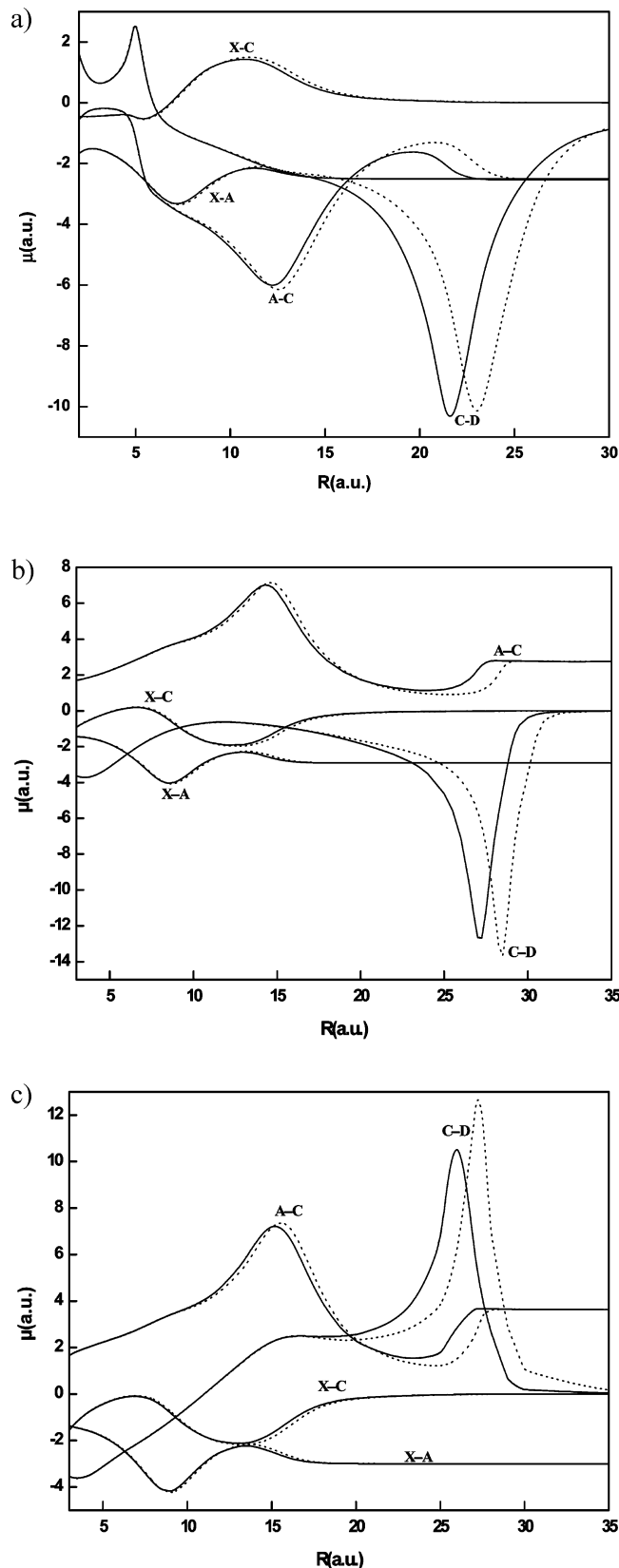


Figure 7. (a) Transition adiabatic dipole moment X–A, X–C, A–C and C–D with (dotted line) and without (solid line) hydrogen electronic affinity correction of the NaH molecule, as a function of the internuclear distance (all in au). (b) Same as panel a but for KH molecule. (c) Same as panel a but for RbH molecule.

are illustrated in Figures 7a, 7b and 7c for the coupled pairs X–A, X–C, A–C and C–D. These adiabatic transition dipoles are imprinted by the ionic curve as can be seen by their changes

when the ionic curve is modified (improved results using the ionic curve corrected for the asymptotic H electron affinity error are reported with dots in Figures 7a, 7b and 7c).

Consistent with the A–C potential curve’s avoided crossing around 16 bohr and also with the related crossing of the permanent dipoles of the A and C states, the X–A and X–C transition dipoles present an avoided crossing at these distances while the A–C transition dipole shows a peak. This behavior can be understood recalling that, around 16 bohr, the A and C states exchange their ionic character while the X state keeps its neutral character. This change in the electronic wave function generates a peak in the A–C transition dipole around 16 bohr as it does also for the radial coupling.

Similarly, the large peak in the C–D transition dipole curve is related to the C–D potential curve’s avoided crossing around 20 bohr; being less avoided, the peak is less wide and higher compared to the A–C case. The behavior of these transition dipole moment matrix elements illustrates the well-known relation between radial coupling and dipole operators, a relation which allowed in a different context the introduction of the electron translation factors. Asymptotically, the X, A, C and D states reach the atomic states of each atom, and the transition dipole reaches the corresponding atomic transitions.

5. Experimental Suggestions

The rather unusual behavior of the excited adiabatic ${}^1\Sigma^+$ states could lead to interesting effects accessible to experimental spectroscopic techniques. There are experimental results on the $X^1\Sigma^+$ and $A^1\Sigma^+$ states only,¹⁰ nothing on the higher ones. However, as in LiH, all of them present a well nearly as deep as the interval between the asymptotic levels. The well minimum moves toward larger interatomic distances as one goes higher in the series and the large distance branch of the well is due to the ionic curve which becomes flatter and flatter as $1/R$. Because of their wide extension, these wells trap a huge number of vibrational levels. In addition to this principal well, which exists for all states whose asymptote is below the ionic X^+H^- ($X = Na, K$ and Rb) one, there are also other wells, less deep and at short interatomic nuclear distances.

In particular, the E and F states present such a well in the Franck–Condon zone of the ground state and could thus be accessible by photoexcitation. The shape of these double wells suggests interesting spectroscopy and dynamics. Since these highly excited states are embedded in a manifold of continua and bound states, strong vibronic effects can be also expected, as predicted and observed^{11,22} for LiH. Work is in progress to determine, with the help of the present nonadiabatic and adiabatic data, conventional and beyond Born–Oppenheimer spectroscopy, including radiative and nonradiative lifetimes, adiabatic corrections and vibronic shifts. Another interesting point is that the R -dependence of the dipole moments can be experimentally derived if the expectation value of the dipole is measured for a sufficiently large number of vibrational levels.

Thus, when measured for various adiabatic states, such information should lead to an experimental determination of the nonadiabatic neutral–ionic crossing and to the related avoided crossings for the potential curves. Another interesting aspect of the present results is related to the outer repulsive branch of the wells of the excited states, corresponding to the ionic species. It exhibits a considerable dipole (a few tenths of atomic unit) due to the prominent charge separation in the ionic state. These unusually large values for the dipole moments should lead to interesting physical effects and to specific signatures, in particular, for the infrared spectrum.

6. Conclusions

Accurate adiabatic and nonadiabatic potential curves have been derived from the ground and excited states of the XH ($X = \text{Na, K, Rb}$) molecule. They result from the use of a nonempirical pseudopotential allowing for a large basis set, full valence CISD (singles–doubles configuration interaction) techniques, operatorial core–valence correlation, and an efficient diabaticization procedure which permit reliable corrections. These excited states are probably described with a similar precision. The surprising shape of the nonadiabatic neutral curves has been analyzed and interpreted from physical arguments. The remarkable accuracy of these results both for individual states and transitions confirms the interest of such ab initio studies and grounds this methodology for the theoretical study of heavy alkali hydrides where all-electron calculations are faced with severe limitations. Our study emphasizes the importance of the accuracy of the ionic state and indeed of the H electron affinity in order to get accurate spectroscopic constants as fundamental as the binding energy of the ground state or the vibrational spacing for the A state.

We have also presented the permanent dipole moments of XH ($X = \text{Na, K, Rb}$) molecule in both the adiabatic and nonadiabatic representations, for a complete manifold of low-lying $^1\Sigma^+$ states and for a large range of internuclear distances. For the nonadiabatic ionic state, the dipole behaves as a straight line.

For the adiabatic states, we have curves which relay each other to this line, illustrating their ionic imprint. These results can be easily understood from the physical nature of the nonadiabatic states and they shed light on the interplay between the ionic and neutral species that dominate the alkali hydride potential curves. Consequently, we suggest determining experimentally the location and width of these avoided crossings.

Acknowledgment. The study was supported by the Research Center of the College of Science at the King Saud University.

References and Notes

- (1) Boutalib, A.; Gadea, F. X. *J. Chem. Phys.* **1992**, *97*, 1144.
- (2) Lepetit, B.; LeDourneuf, M.; Launay, J. M.; Gadea, F. X. *Chem. Phys. Lett.* **1987**, *135*, 377.
- (3) Chambaud, G.; Lévy, B. *J. Phys. B* **1989**, *22*, 3155.
- (4) Pelissier, M.; Komih, N.; Daudey, J. P. *J. Comput. Chem.* **1988**, *9*, 298.

- (5) Peckeris, C. L. *Phys. Rev.* **1962**, *126*, 1470.
- (6) Malrieu, J. P.; Maynaud, D.; Daudey, J. P. *Phys. Rev. B* **1984**, *30*, 1817.
- (7) Garcia, V. M.; Caballol, R.; Malrieu, J. P. *J. Chem. Phys.* **1998**, *109*, 504.
- (8) Jeung, G. H.; Daudey, J. P.; Malrieu, J. P. *J. Phys. B* **1983**, *16*, 699.
- (9) Stwalley, W. C.; Zemke, W. T. *J. Phys. Chem. Ref. Data* **1993**, *22*, 87.
- (10) Stwalley, W. C.; Zemke, W. T.; Yang, S. C. *J. Phys. Chem. Ref. Data* **1991**, *20*, 153.
- (11) Lee, H. S.; Lee, Y. S.; Jeung, G. H. *Chem. Phys. Lett.* **2000**, *325*, 46.
- (12) Gemperle, F.; Gadea, F. X. *J. Chem. Phys.* **1999**, *110*, 111.
- (13) Gadea, F. X.; Boutalib, A. *J. Phys. B* **1993**, *26*, 61.
- (14) Berriche, H.; Gadea, F. X. *Chem. Phys. Lett.* **1995**, *247*, 85.
- (15) Croft, H.; Dickinson, A. S.; Gadea, F. X. *J. Phys. B* **1999**, *32*, 81.
- (16) Croft, H.; Dickinson, A. S.; Gadea, F. X. *Mon. Not. R. Astron. Soc.* **1999**, *304*, 327.
- (17) Dickinson, A. S.; Gadea, F. X. *Mon. Not. R. Astron. Soc.* **2000**, *318*, 1227.
- (18) Gadea, F. X.; Gemperle, F.; Berriche, H.; Villarreal, P.; Delgado-Barrio, G. *J. Phys. B* **1997**, *30*, L427.
- (19) Gemperle, F.; Gadea, F. X. *Europhys. Lett.* **1999**, *48*, 513.
- (20) Gadea, F. X.; Berriche, H.; Roncero, O.; Villarreal, P.; Delgado-Barrio, G. *J. Chem. Phys.* **1997**, *107*, 10515.
- (21) Yiannopoulou, A.; Jeung, G. H.; Lee, H. S.; Lee, Y. S. *Phys. Rev. A* **1999**, *59*, 1178.
- (22) Dickinson, A. S.; Poteau, R.; Gadea, F. X. *J. Phys. B* **1999**, *32*, 5451.
- (23) Leininger, T.; Gadea, F. X.; Dickinson, A. S. *J. Phys. B* **2000**, *33*, 1805.
- (24) Müller, W.; Flesh, J.; Meyer, W. *J. Chem. Phys.* **1984**, *80*, 3297.
- (25) (a) Durand, Ph.; Barthelat, J. C. *Theor. Chem. Acta* **1975**, *38*, 283.
- (b) Barthelat, J. C.; Durand, Ph. *Gazz. Chim. Ital.* **1978**, *108*, 225.
- (26) Foucrault, M.; Millie, Ph.; Daudey, J. P. *J. Chem. Phys.* **1988**, *96*, 1257.
- (27) Moore, C. E. *Atomic Energy Levels* NBS, USGPO: Washington, DC, 1971.
- (28) Gadea, F. X. Thèse d'état, Université Paul Sabatier, Toulouse, 1987.
- (29) Gadea, F. X.; Pelissier, M. *J. Chem. Phys.* **1990**, *93*, 545.
- (30) Romero, T.; Aguilar, A.; Gadea, F. X. *J. Chem. Phys.* **1999**, *110*, 16219.
- (31) Gadea, F. X. *Phys. Rev. A* **1991**, *43*, 1160.
- (32) Fermi, E. *Nuovo Cimento* **1934**, *11*, 157.
- (33) Omont, A. *J. Phys. (Paris)* **1977**, *38*, 1343.
- (34) Jeung, G. H.; Daudey, J. P.; Malrieu, J. P. *J. Phys. B* **1983**, *16*, 699.
- (35) Lee, H. S.; Lee, Y. S.; Jeung, G.-H. *Chem. Phys. Lett.* **2000**, *325*, 46.
- (36) Dolg, M. *Mol. Phys.* **1996**, *93*, 141.
- (37) Fuentealba, P.; Reyes, O.; Stoll, H.; Preuss, H. *J. Chem. Phys.* **1987**, *87*, 5338.
- (38) Olsen, R. E.; Liu, B. *J. Chem. Phys.* **1980**, *73*, 2817.

JP9040138